

CMB constraints on dark matter phenomenology via reheating in Minimal plateau inflation

Debaprasad Maity^{1,*} and Pankaj Saha^{1,†}

¹*Department of Physics, Indian Institute of Technology Guwahati.*

Guwahati, Assam, India

(Dated: December 3, 2024)

Abstract

Dynamics of non-standard inflation potential has been gaining significant interest in recent times. Based on our recent proposal on supergravity inspired minimal inflationary cosmologies for non-polynomial plateau potential, in this paper, we perform a detailed reheating constraints analysis considering the perturbative decay of inflaton to radiation and the dark matter. Our present study focuses on constraining the models under consideration through reheating phase supplemented by CMB anisotropy and current dark matter abundance. We have solved the appropriate set of homogeneous Boltzmann equations for decaying inflaton, radiation, and the dark matter starting from the end of inflation till freezing in of dark matter and found stringent constraints on the model parameters. Given the inflationary power spectrum n_s from PLANCK and particular inflationary model, we analyze in detail the constraints on dark matter parameter space namely the dark matter annihilation cross-section ($\langle\sigma|v|\rangle$), mass (M_X) of a single component dark matter produced from decaying inflaton.

Keywords:

*Electronic address: debu@iitg.ac.in

†Electronic address: pankaj.saha@iitg.ac.in

Contents

I. Introduction	3
II. Brief account on minimal inflationary potentials and their origin	4
A. $V_{min}(\phi)$ from Supergravity	5
B. $V_{min}(\phi)$ from non-minimal scalar tensor theory	6
III. CMB to dark matter phenomenology via reheating	8
1. The Boltzmann Equations during reheating with general inflaton equation of state	9
2. The early time solution and the maximum temperature for general	
$\omega_\phi = (n - 2)/(n + 2)$	11
3. Dark matter relic abundance and its (T_{re}, T_{max}) dependence	11
A. Connection between CMB and dark matter: Methodology	12
1. Numerical results, constraints on the model	14
2. Results and constraints: Model n=2	16
3. Results and constraints: Model n=4	18
4. Results and constraints: Model n=6	19
5. Results and constraints: Model n=8	20
IV. Conclusions and future directions	22
V. Acknowledgement	25
References	25

I. INTRODUCTION

Reheating is one of the important phases of the universe evolution. This is the phase during which all the matter fields of the current universe are assumed to have been produced from the oscillating inflaton field. Therefore, in order to make any connection with the present universe, the mechanism of inflation [1–3] is important. For this, model building is an important part of the current research in inflationary cosmology. Over the years a lot of models have been put forward [4], to explain the observations [5]. The simplest model of inflation is known to be governed by a single scalar field with power-law potential. However, with the increasing precision of observation, those models turned out to be disfavored. As an alternative, a class of single field α attractor [6] models have been recently proposed with a modified form of the potential which not only fits well with the observation but also unifies different existing models in a single fold. In view to reconcile power law potentials with observations, we proposed [7] another class of models with a plateau potential in the large field limit while the potential during reheating is simply governed by the leading power-law term: $V(\phi) \propto \phi^n$. Inflationary dynamics have already been studied in detail in the aforementioned references. As emphasized in the beginning, in this paper we will focus on reheating period. Depending upon the inflaton coupling with the decaying fields, reheating phase can be both perturbative [8] and/or non-perturbative [9]. Usually, the reheating period is less constrained by the cosmological observation. Interestingly in the recent papers [10–12, 14], an important connection has been established between the cosmic microwave background (CMB) and reheating phase. Analysis of those papers was based on one of the important assumptions that the reheating phase is governed by an effective single fluid with a time independent equation of state. Recently we proposed a possible generalization of their work by taking into account the explicit decay of inflaton during reheating. However, we assume the decay to be perturbative. This approach has an interesting consequence that we can go beyond the usual reheating phenomena, and shed light on how one can constrain the dark matter parameter space through CMB anisotropy. Therefore, following the formalism developed in [15, 29], we study the CMB constraints on the inflation model, the reheating phase, and the dark matter production during reheating for our recently proposed minimal inflationary models.

We organize our paper as follows: In section-II, we briefly review the minimal inflationary cosmological models studied in detail in [29]. After the end of inflation, generically the inflaton starts to have coherent oscillation at the minimum of the potential, during which the universe will undergo reheating phase. We also compute the effective equation of state of the oscillating inflaton for our subsequent studies. In section-III, we have studied the reheating constraints from CMB and

production of a heavy dark matter particle during reheating. Finally, we concluded and discussed our future work.

II. BRIEF ACCOUNT ON MINIMAL INFLATIONARY POTENTIALS AND THEIR ORIGIN

As we have discussed in this section we will briefly review the inflationary models proposed in [7] specifically mentioning the scalar-spectral index in terms of our model parameters. The non-polynomial plateau potential looks like the following form,

$$V_{min}(\phi) = \begin{cases} \lambda \frac{m^{4-n} \phi^n}{1 + \left(\frac{\phi}{\phi_*}\right)^n} \\ \lambda \frac{m^{4-n} \phi^n}{\left(1 + \left(\frac{\phi}{\phi_*}\right)^2\right)^{\frac{n}{2}}}, \end{cases} \quad (1)$$

(m or λ, n) are our model parameters. λ is reserved for $n = 4$, [15]. For other value of n , we $\lambda = 1$. The potential is so constructed that for large value of ϕ_* , it becomes approximately shift symmetric which is usually dubbed as the plateau potential. The scale $\Lambda = \lambda m^{4-n} \phi_*^n$ can be associated with the inflationary scale which is essentially the height of the potential during inflation. Considering $\phi_* \leq \mathcal{O}(1)$ in unit of M_p , a general expression for the scalar spectral index and the tensor to scalar ratio are calculated as,

$$1 - n_s = \begin{cases} \frac{2(n+1)}{(n+2)} \frac{1}{N} \\ \frac{3}{2N} \end{cases} ; \quad r = \begin{cases} 8n^2 \left(\frac{\phi_*}{M_p}\right)^{\frac{2n}{(n+2)}} \frac{1}{[n(n+2)]^{\frac{2(n+1)}{(n+2)}} N^{\frac{2(n+1)}{(n+2)}}} \\ \frac{\phi_*}{M_p} \frac{n \frac{1}{2}}{N^{\frac{3}{2}}} \end{cases} \quad (2)$$

For $\phi_* < \mathcal{O}(\infty)$, it turns out that the tensor to scalar ratio explicitly depends upon the inflationary scale itself. In all the above expressions, we have taken large- N limit. However, it is important to remember that the aforementioned series expansion is inapplicable for large $\phi_* > 1 M_p$, which has already been discussed in our previous paper. At this point we also would like to stress an important fact that in large n limit, for Type-I potential above cosmological observables takes the following form,

$$1 - n_s \rightarrow \frac{2}{N}; \quad r \rightarrow 8 \left(\frac{\phi_*}{M_p}\right)^2 \frac{1}{N^2}, \quad (3)$$

which is precisely the prediction of α -attractor model [6]. What we have seen from the detailed analysis is the perfect fit of our models with the experimental results for a wide range of parameters. However, the most difficult point would be to understand the selection criteria based on which one can identify a specific model. For all the models we have similar predictions with the same number

of external parameters. We all know that usual power-law potential with single parameter which is the mass of the inflaton, always predicts large tensor to scalar ratio. Therefore, in terms of inflation model building increasing the number of control parameters may be necessary towards understanding the observation. With this motivation in mind, we had proposed the aforementioned models. In the following sub-sections let us briefly provide the origin of the aforementioned models based on supergravity and non-minimal scalar tensor theory.

A. $V_{min}(\phi)$ from Supergravity

Here we will present a brief account of supergravity realization of our model potential which we recently understood [7]. We consider the following form of the Kähler and superpotential with three chiral superfields S and $\{\Phi_1, \Phi_2\}$

$$\begin{aligned} W &= \frac{\phi_* S^2}{2} (\Phi_1^p - \Phi_2^p) \\ K &= |S|^2 + |\Phi_1|^2 + |\Phi_2|^2, \end{aligned} \quad (4)$$

Assuming a suitable R -symmetry, one arrives at the following form of F-term potential at its minimum with $|\Phi_1| = |\Phi_2| \equiv \phi$, where ϕ is a real scalar field as,

$$V_F = e^{\frac{\phi}{M_p^2}} |S|^4 p^2 \left(\frac{\phi}{\phi_*} \right)^{2p-2} \quad (5)$$

In order to obtain our minimal form of the potential, we also consider D-term potential coming from the appropriate form of the gauge kinetic function, following the references [13, 16]

$$V_D = \frac{1}{2} \left(|S|^2 - \sqrt{2} M^2 \right)^2. \quad (6)$$

Hence total potential turns out to be

$$V_T = e^{\frac{\phi}{M_p^2}} |S|^4 p^2 \left(\frac{\phi}{\phi_*} \right)^{2p-2} + \frac{1}{2} \left(|S|^2 - \sqrt{2} M^2 \right)^2 \quad (7)$$

Minimizing the potential along the S direction reduces the scalar potential into the following simple form

$$V_{sugra}(\phi) = \frac{m^{4-n} \phi^n}{\exp\left(-\frac{\phi^2}{2M_p^2}\right) + \left(\frac{\phi}{\phi_*}\right)^n} \quad (8)$$

Where $n = 2(p-1)$ and $m = (M^4 \phi_*^{-n})^{1/(4-n)}$. In the limit $\phi_* < M_p$, this plateau potential reduces to one of our minimal plateau potentials as follows,

$$V_{min}(\phi) = \frac{m^{4-n} \phi^n}{1 + \left(\frac{\phi}{\phi_*}\right)^n}. \quad (9)$$

Hence from our supergravity model, we obtained the type-I potential in a limit where ϕ_* is sub-Planckian. In next sub-subsection we discuss about the same form of the potential in the super-Planckian regime of ϕ^* considering the non-minimal scalar tensor theory.

B. $V_{min}(\phi)$ from non-minimal scalar tensor theory

In the phenomenological minimal plateau potential, we considered non-polynomial type function, which may be difficult to justify in the perturbative field theory point of view. In this section, we will briefly describe how we can arrive at the same form of the non-polynomial potential from polynomial function with additional conformal transformation [17, 18]. Let us begin with the following non-minimally coupled scalar-tensor theory,

$$S_J = \int d^4x \sqrt{-g} \left[\frac{\Omega(\varphi)}{2} M_p^2 R - \frac{\Omega(\varphi)}{2} g^{\mu\nu} \partial_\mu \varphi \partial_\nu \varphi - V(\varphi) \right], \quad (10)$$

where, $\Omega(\varphi)$ is arbitrary function of a scalar field φ . Applying the conformal transformation, $\tilde{g}_{\mu\nu} = \Omega(\varphi) g_{\mu\nu}$, one gets the Einstein frame action [26] as follows,

$$S_E = \int d^4x \sqrt{-\tilde{g}} \left[\frac{M_p^2}{2} \tilde{R} - \frac{1}{2} F^2(\varphi) \tilde{g}^{\mu\nu} \partial_\mu \varphi \partial_\nu \varphi - \tilde{V}(\varphi) \right], \quad (11)$$

Where

$$F^2(\varphi) = \frac{3M_p^2}{2} \frac{\Omega'^2(\varphi)}{\Omega^2(\varphi)} + 1 \quad ; \quad \tilde{V}(\varphi) = \frac{V(\varphi)}{\Omega^2(\varphi)} \quad (12)$$

Now, we choose the following two possible polynomial functional form of coupling functions [27, 28],

$$\Omega^2(\varphi) = \begin{cases} 1 + \xi \left(\frac{\varphi}{M_p}\right)^n \\ \left[1 + \xi \left(\frac{\varphi}{M_p}\right)^2\right]^{\frac{n}{2}} \end{cases} \quad (13)$$

Therefore, applying (13), we find F and \tilde{V} as,

$$F^2(\varphi) = \begin{cases} \frac{3n^2 \xi^2 \left(\frac{\varphi}{M_p}\right)^{2(n-1)}}{8 \left[1 + \xi \left(\frac{\varphi}{M_p}\right)^n\right]^2} + 1 \\ \frac{3n^2 \xi^2 \left(\frac{\varphi}{M_p}\right)^2}{8 \left[1 + \xi \left(\frac{\varphi}{M_p}\right)^2\right]^2} + 1 \end{cases} \quad ; \quad \tilde{V}(\varphi) = \begin{cases} \frac{V(\varphi)}{1 + \xi \left(\frac{\varphi}{M_p}\right)^n} \\ \frac{V(\varphi)}{\left[1 + \xi \left(\frac{\varphi}{M_p}\right)^2\right]^{\frac{n}{2}}} \end{cases} \quad (14)$$

We use the following field redefinition

$$\frac{d\phi}{d\varphi} = F(\varphi) \quad (15)$$

$\frac{\phi_*}{M_p}$	n	Model I		Model II	
		n_s	r	n_s	r
0.01	2	0.969	4×10^{-5}	0.969	4×10^{-5}
	4	0.966	2×10^{-6}	0.969	5×10^{-5}
	6	0.965	3×10^{-7}	0.969	7×10^{-5}
	8	0.964	1×10^{-7}	0.969	8×10^{-5}
1	2	0.969	4×10^{-3}	0.969	4×10^{-3}
	4	0.966	9.6×10^{-4}	0.969	6×10^{-3}
	6	0.964	3.5×10^{-4}	0.969	7×10^{-3}
	8	0.964	1.7×10^{-4}	0.969	8×10^{-3}

TABLE I: Sample values of (n_s, r) are given for two values of $\phi_* = (0.01, 1)M_p$ corresponding to small field and large field inflation respectively.

At this point we need to integrate eq.(15), to figure the canonical scalar field potential in terms of new field. However, for entire range of parameter ξ , we will not be able to reproduce our minimal potential. Therefore, we restrict in the weak coupling $\xi \ll 1$, $F \sim 1$, eq(15) regime and arrive at

$$V_{min}(\phi) = \begin{cases} \frac{\lambda m^{4-n} \phi^n}{1 + \left(\frac{\phi}{\phi_*}\right)^n} \\ \frac{\lambda m^{4-n} \phi^n}{\left[1 + \left(\frac{\phi}{\phi_*}\right)^2\right]^{\frac{n}{2}}}, \end{cases} \quad (16)$$

where, we identify ϕ_* as $M_p/\xi^{\frac{1}{n}}$ for Type-I potential and $M_p/\xi^{\frac{1}{2}}$ for type-II potential. Therefore, in the weak coupling regime, $\xi \ll 1$ or $\phi_* > 1$, the non-minimal scalar tensor theory can give rise to a large class of minimal cosmologies such as ours which do not belong the α -attractor model.

In any case, the main goal of our previous and the present work is to understand the phenomenological models based on observations. In this regard, one of the important observable quantities which helps us to fix one of the parameters is the amplitude of the scalar field fluctuation which is defined as scalar power spectrum, $\mathcal{P}_{\mathcal{R}} = 2.4 \times 10^{-9}$, based on PLANCK normalization. The value is fixed at the pivot scale $k/a_0 = 0.05 Mpc^{-1}$. Corresponding observed scalar spectral index is $n_s = 0.9682 \pm 0.0062$, and the upper limit on the tensor to scalar ratio is set to be $r < 0.11$. In table-(I), we have given some sample values of all the cosmologically relevant quantities for different values of parameters. Our main goal of this paper is to study the reheating dynamics and consequently the dark matter phenomenological constraints based on the formalism developed in [10] and its generalization proposed in [29]. We will show how the inflationary scale ϕ_* plays important role in determining the reheating temperature and consequently its influence on the dark matter parameter space. The Only assumption we will make in our analysis is the perturbative

decay of the inflaton field into radiation and radiation into the dark matter field. We also would like to mention that all the results of the present paper will be based on the first model-I. The similar analysis can be done for the other one, and the qualitative results will remain same.

III. CMB TO DARK MATTER PHENOMENOLOGY VIA REHEATING

It has been a general consensus that the inflation phase must be followed by the reheating phase. During this phase, the inflaton field is assumed to decay into various daughter fields such as radiation, dark matter particles, etc. The quantity which characterizes this phase is known as the reheating temperature (T_{re}) and its duration (N_{re}). Reheating temperature is defined at the instant when the inflaton decay rate equals the universe expansion rate and the radiation domination sets in. Being not an observable quantity, the reheating temperature is usually considered as a free parameter where its upper value could be as high as the GUT scale and the lower value is fixed by the requirement of successful Big Bang Nucleosynthesis. However, it has been established in the recent reference [10] that not just inflationary phase but also the reheating phase can be constrained by CMB anisotropy. Since then, there has been a surge of research work in this direction[11, 12, 30–36]. The inherent assumption in all those works is that the inflaton field converts into radiation instantaneously at the end of reheating and the effective fluid describing the reheating dynamics is parameterized by an average equation of state parameter. In our recent work[15, 29], we have shown that by relaxing the aforementioned assumptions we not only can constrain the inflationary model but also shed light on the dark matter phenomenology. Through our analysis, we were able to connect the current dark matter relic abundance with the temperature anisotropy in CMB. In this paper, we will follow the aforementioned formalism developed in [29] and generalize it for the arbitrary equation of state of the inflaton during inflation. In our model, during reheating phase the inflaton potential can be approximated as $V(\phi) \propto \phi^n$ such that the equation of state of the oscillating inflaton can be approximated as $w_\phi = (n - 2)/(n + 2)$. An illustration of how CMB constraints the reheating temperature as well as how the equation of state parameter play a significant role controlling the reheating period is presented in fig.(1). It is also clear from the figure that for a particular scale and the inflaton equation of state during reheating we have maximum possible value of n_s^{max} for $w_{eff} < 1/3$ and minimum possible value of n_s^{min} for $w_{eff} > 1/3$. Where w_{eff} is the effective equation of state during reheating. However, for our case, we will consider explicit decay of inflation to radiation and dark matter during reheating. Therefore, the existence of (n_s^{max}, n_s^{min}) will depend on the equation of state of inflaton w_ϕ itself. It also implies the existence of maximum reheating temperature T_{re}^{max} . Interestingly we will see that the maximum reheating

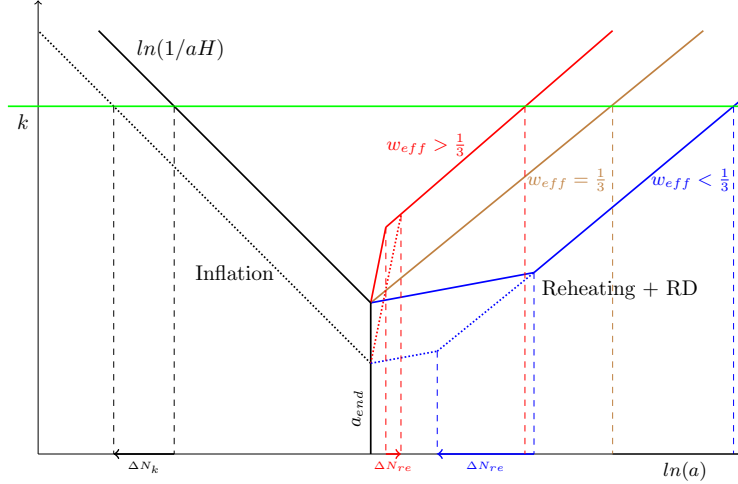


FIG. 1: Evolution of the comoving Hubble horizon starting from inflation (left side black lines), reheating (intermediate lines), radiation domination up to the present time (the shorter period of matter domination and the current dark energy domination is not shown as they don't affect the qualitative conclusion). During the reheating phase when the effective equation of state $w_{eff} = 1/3$, the evolution is indistinguishable from radiation dominated phase as shown in solid brown line. This fact makes reheating parameters (N_{re}, T_{re}) indeterministic as observed in [10]. The evolution with $w_{eff} < 1/3$ is shown in blue intermediate lines while that of $w_{eff} > 1/3$ is shown in red intermediate lines. Increase in n_s implies going from solid black line to dotted black line adding extra e-folding number ΔN_k for horizon crossing of a particular CMB mode k . It is clear from the figure for $w_{eff} < 1/3$, increasing n_s will result in decreasing reheating e-folding number during reheating N_{re} thereby increasing reheating temperature T_{re} . While for $w_{eff} > 1/3$ it will just be the opposite. Hence, one can clearly expect an upper bound on n_s for a particular inflation model with $w_{\phi} < 1/3$ where the intermediate line closes indicating an instantaneous reheating with maximum possible reheating temperature. On the other hand for models with $w_{\phi} > 1/3$, one expects a lower bound on n_s . The bound on the other end of n_s for both the cases will be from the condition of minimum reheating temperature for a successful BBN.

temperature T_{re}^{max} does not depend on a particular model under consideration.

1. The Boltzmann Equations during reheating with general inflaton equation of state

We will consider three component universe consisting of inflaton (ρ_{ϕ}), radiation (ρ_R) and a massive dark matter particle with the number density (n_X). For simplicity, we consider dark matter particle production only from radiation annihilation. For the general equation of state of inflaton, we will work with the following rescaled variables,

$$\Phi = \frac{\rho_{\phi} a^{3(1+w_{\phi})}}{m_{\phi}^{(1-3w_{\phi})}}; \quad R = \rho_R a^4; \quad X = n_X a^3. \quad (17)$$

The Boltzmann equations[29, 37] in the rescaled variables with the time variable $A = a/a_I$ reduces to,

$$\begin{aligned}\frac{d\Phi}{dA} &= -c_1(1+w_\phi)\frac{A^{1/2}\Phi}{\mathbb{H}}; \\ \frac{dR}{dA} &= c_1(1+w_\phi)\frac{A^{3(1-2w_\phi)/2}}{\mathbb{H}}\Phi + c_2\frac{A^{-3/2}2\langle E_X\rangle\langle\sigma v\rangle M_{pl}}{\mathbb{H}}(X^2 - X_{eq}^2); \\ \frac{dX}{dA} &= -c_2\frac{A^{-5/2}2\langle E_X\rangle\langle\sigma v\rangle M_{pl}}{\mathbb{H}}(X^2 - X_{eq}^2);\end{aligned}\tag{18}$$

Where, $\mathbb{H} = (\Phi/A^{3w_\phi} + R/A + X\langle E_X\rangle/m_\phi)^{1/2}$ is the Hubble expansion rate and the constants c_1 and c_2 are given by

$$c_1 = \sqrt{3}\frac{M_P\Gamma}{m_\phi^2}, \quad c_2 = \sqrt{\frac{3}{8\pi}}\tag{19}$$

Here, $M_{pl}(= \sqrt{8\pi}M_p)$ is the Planck mass. $\langle E_X\rangle = \rho_X/n_X$ is the average energy density of the X-particle which we identify as the candidate dark matter. X_{eq} is the equilibrium (comoving-)number density of the dark matter of mass M_X if it is in equilibrium with background thermal bath at temperature T . Γ is the inflaton decay rate. We assume the dark matter has an internal degree of freedom g . Since we want to study all range of mass of the dark matter, we use the relativistic form of the equilibrium distribution function with the modified Bessel function of the second kind as[37, 38]

$$X_{eq} = \frac{gT^3}{2\pi^2}\left(\frac{M_X}{T}\right)^2 K_2\left(\frac{M_X}{T}\right)\left(\frac{A}{m_\phi}\right)^3\tag{20}$$

In all the above equation we introduce an arbitrary mass scale m_ϕ for convenience in numerical computation. We will take it as the Hubble constant at the end of inflation. At this point, let us emphasize that our analysis is purely perturbative. However the non-perturbative effects may have an important role, we left it for our future studies. In order to solve, the above set of Boltzmann equation, we set the initial condition at the end of inflation as,

$$\Phi(1) = \frac{3}{8\pi}\frac{M_{pl}^2 H_I^2}{m_\phi^4}; \quad R(1) = X(1) = 0.\tag{21}$$

Where the initial Hubble expansion $H_I^2 = (8\pi/3M_{pl}^2)\rho_{\phi,end}$. The set of Boltzmann equations can now be easily solved provided we know the inflaton decay with and the annihilation cross section. The reheating temperature of the universe is identified at the instant of $H(t) = \Gamma_\phi$, when all the inflaton field energy is instantaneously converted into the radiation field. However, in general, this is not true. At any instant of time during the evolution, the temperature of our universe is identified with the radiation temperature with $T \equiv T_{rad} = [30/(\pi^2 g_*)]^{1/4} \rho_R^{1/4}$. The thermally averaged annihilation cross section of the dark matter from the radiation is $\langle\sigma v\rangle$ [37]. We will be using this as a free parameter in our subsequent numerical analysis.

2. *The early time solution and the maximum temperature for general $\omega_\phi = (n - 2)/(n + 2)$*

Before we resort to the numerical solution to find the connection among the CMB anisotropy and the dark matter abundance, let us compute an analytic expression for the maximum possible temperature during reheating phase for general equation of state of the inflaton field. In the early phase of the reheating stage ($H \gg \Gamma_\phi$), considering the initial condition $R(A_I) \simeq X(A_I) \simeq 0$ eq.(18) can be solved as

$$\frac{dR}{dA} \simeq c_1(1 + w_\phi)\Phi_I^{\frac{1}{2}}A^{\frac{3}{2}(1-w_\phi)} \implies R \simeq 2c_1 \left(\frac{1 + w_\phi}{5 - 3w_\phi} \right) \left[A^{\frac{5-3w_\phi}{2}} - A_I^{\frac{5-3w_\phi}{2}} \right]. \quad (22)$$

Therefore, by using the above solution and using the definition of temperature in terms of the radiation density, one arrive at the following expression

$$T = \left[\frac{60c_1}{g_*\pi^2} \frac{1 + w_\phi}{5 - 3w_\phi} \right]^{\frac{1}{4}} m_\phi \left(\frac{\Phi_I}{A_I^{3(1+w_\phi)}} \right)^{\frac{1}{8}} \left[\left(\frac{A}{A_I} \right)^{-\frac{3}{2}(1+w_\phi)} - \left(\frac{A}{A_I} \right)^{-4} \right]^{\frac{1}{4}} \quad (23)$$

By using the the eq.(21), the maximum temperature can be found as

$$T_{max} = \left[\frac{60c_1}{g_*\pi^2} \frac{1 + w_\phi}{5 - 3w_\phi} \right]^{\frac{1}{4}} m_\phi^{\frac{1}{2}} \left(\frac{3}{8\pi} \frac{M_{pl}^2 H_I^2}{A_I^{3(1+w_\phi)}} \right)^{\frac{1}{8}} \left[\left(\frac{8}{3(1 + w_\phi)} \right)^{-\frac{3(1+w_\phi)}{5-3w_\phi}} - \left(\frac{8}{3(1 + w_\phi)} \right)^{-\frac{8}{5-3w_\phi}} \right] \quad (24)$$

In the following numerical analysis for the dark matter abundance, we will find maximum temperature plays an important role in constraining the dark matter parameter space. The essential idea behind this temperature is that as the reheating temperature is measured at a later stage of reheating, the radiation production commences at the very early stage. As one can clearly see the non-trivial dependence of the temperature on the inflaton equation of state parameter (ω_ϕ) and the inflaton decay constant Γ_ϕ . Depending upon the initial value of Hubble rate which has a direct connection with the CMB anisotropy, the maximum temperature can be many order higher than the reheating temperature[37, 39, 40]. Therefore, this maximum temperature will play as an intermediate scale between the inflationary energy scale and the reheating temperature. Subsequently we show how this will effect the dark matter production mechanism during depending upon the dark matter mass.

3. *Dark matter relic abundance and its (T_{re}, T_{max}) dependence*

As we have emphasized already, we will describe how the present dark matter abundance is controlled by the CMB anisotropy through the inflationary model and its subsequent reheating phase. The present dark matter abundance parametrized by the normalized density parameter Ω_χ

can be expressed in terms of present day radiation abundance Ω_R ($\Omega_R h^2 = 4.3 \times 10^{-5}$), as follows

$$\Omega_X h^2 = \langle E_X \rangle \frac{X(T_F)}{R(T_F)} \frac{T_F}{T_{now}} \frac{A_F}{m_\phi} \Omega_R h^2 \quad (25)$$

Where, T_F is the temperature at very late time when dark matter and radiation comoving energy densities became constant. The current CMB temperature is given by $T_{now} = 2.35 \times 10^{-13} GeV$. For our subsequent discussions, it is important to know the behavior of the dark matter abundance in terms of reheating parameters ($T_{re}, M_X, \langle \sigma v \rangle$). The analytic expressions for the dark matter abundance for different dark matter mass M_X can be calculated following the references [37] (See also [41, 42] for an alternative derivation). As we have considered a generic equation of state parameter for the inflaton, we are interested in the generalized expression for dark matter abundance for arbitrary w_ϕ . The dependence of relic abundance on reheating temperature, the dark matter mass, and annihilation cross section can be expressed as

$$\Omega_X h^2 \propto \langle \sigma |v| \rangle M_X^4 \text{Exp} \left[-\frac{E(w_\phi) M_X}{T_{max}} \right] \quad \text{for } M_X \gtrsim T_{max} \quad (26)$$

$$\Omega_X h^2 \propto \langle \sigma v \rangle \frac{T_{re}^{\frac{7+3w_\phi}{1+w_\phi}}}{M_X^{\frac{9-7w_\phi}{2(1+w_\phi)}}} \quad \text{for } T_{max} > M_X > T_{re}. \quad (27)$$

One can particularly notice the non-trivial dependence of w_ϕ for two different dark matter mass range with respect to the T_{max} as derived before. The proportionality factors for the above expressions and $E(w_\phi)$ has a complicated dependence on w_ϕ , which are important for our subsequent discussions. Furthermore, if we consider the dark matter mass to be less than the reheating temperature, the *freeze-in* happens after the reheating is over. For that case the relic abundance can be expressed as [43]

$$\Omega_X h^2 \propto \langle \sigma v \rangle M_X T_{re} \quad \text{When } M_X < T_{re}, \quad (28)$$

For all the above three expressions for the dark matter abundance, we have considered the freeze-in mechanism. This essentially means that dark matter will never reach the equilibrium with the thermal bath. In the literature, these dark matter is known as feebly interacting dark matter (FIMP) [44]. Following our recent work [29], in the next section, we will briefly outline the steps to connect CMB, reheating and dark matter abundance.

A. Connection between CMB and dark matter: Methodology

In this section we will briefly review the methodology developed in [29] which describes the connection between the CMB anisotropy and the dark matter phenomenology. For the canonical

inflation, the important physical quantities are $(N_k, H_k, V_{end}(\phi_k))$ which we have already defined. Since we would like to compute for a specific CMB scale k (CMB pivot scale), all those quantities are expressed as

$$H_k = \frac{\pi M_p \sqrt{r A_s}}{\sqrt{2}} \quad ; \quad N_k = \ln \left(\frac{a_{end}}{a_k} \right) = \int_{\phi_k}^{\phi_{end}} \frac{1}{\sqrt{2\epsilon_V}} \frac{|d\phi|}{M_p}. \quad (29)$$

where (ϕ_{end}) is computed from the condition of end of inflation

$$\epsilon(\phi_{end}) = \frac{1}{2M_p^2} \left(\frac{V'(\phi_{end})}{V(\phi_{end})} \right)^2 = 1, \quad (30)$$

While, the value of the scalar spectral index n_s^k at the horizon crossing of a particular scale k is

$$n_s^k = 1 - 6\epsilon(\phi_k) + 2\eta(\phi_k) \quad (31)$$

Now, the above expression can be inverted to find ϕ_k in terms of the scalar spectral index. This relation provides us the connection between CMB anisotropy and the inflationary dynamics. Thus using this constraint from CMB on inflation, we will set the initial condition for the subsequent reheating dynamics. Next, we will solve the Boltzmann eq.(19) for all the three components of energy densities and also the scale factor a during the reheating phase. For numerical analysis one of the important quantities called reheating e-folding number N_{re} measuring the duration of reheating is computed from the standard definition $N_{re} = \ln(a_{re}/a_{end})$. Where a_{re} is the scale factor at the end of reheating which is defined as

$$H(a_{re})^2 = \frac{\dot{a}_{re}}{a_{re}} = \frac{8\pi}{3M_{Pl}^2} (\rho_\phi(\Gamma, n_s^k, M_X) + \rho_R(\Gamma, n_s^k, M_X) + \rho_X(\Gamma, n_s^k, M_X)) = \Gamma^2. \quad (32)$$

Where each of the energy components is written as an implicit function of reheating parameters and inflationary power spectrum n_s^k as they are the solution of the Boltzmann equations with the initial condition at the end of inflation expressed in eq.(21). This is also the scale factor at which we define the radiation temperature as another important parameter called reheating temperature with the following relation

$$T_{re} \equiv T_{rad}^{end} = [30/\pi^2 g_*(T)]^{1/4} \rho_R(\Gamma, n_s, M_X)^{1/4}. \quad (33)$$

At this point, it is important to note that in the present case the reheating temperature cannot be straightforwardly expressed in terms of inflaton decay width Γ , as can be clearly seen from the above equation. Never the less, the cosmological scale k observed in CMB is originated during inflation at the horizon scale H_k , and then evolved through the subsequent reheating and radiation phase. Therefore, an important relation has been established among $(H_k, T_{re}, N_{re}, T_0)$ in [10], as

$$T_{re} = \left(\frac{43}{11g_{re}} \right)^{\frac{1}{3}} \left(\frac{a_0 T_0}{k} \right) H_k e^{-N_k} e^{-N_{re}}. \quad (34)$$

where $T_0 = 2.725K$ is the present CMB temperature, g_{re} is the effective number of light species, and H_0 is the present value of the Hubble parameter. Hence one gets an important connection among the CMB anisotropy at a particular scale k , inflation and the reheating period through the following equation,

$$\left(\frac{43}{11g_{re}}\right)^{\frac{1}{3}} \left(\frac{a_0 T_0}{k}\right) H_k e^{-N_k} e^{-N_{re}} = [30/\pi^2 g_*(T)]^{1/4} \rho_R(\Gamma, n_s, M_X)^{1/4} \quad (35)$$

However, following the reference [29], in addition to radiation, we also considered the production of dark matter. Therefore, the observation of present dark matter abundance $\Omega_X h^2 = 0.12$ will lead to the following another important connection between CMB anisotropy, reheating and the dark matter phenomenology. Following the relations given in Eqs.(26,27,28), the aforementioned connection are expressed as follows,

$$\begin{aligned} \Omega_X h^2 &\propto \langle \sigma | v \rangle M_X^4 \text{Exp} \left[-\frac{E(w_\phi) M_X}{T_{max}} \right] \quad \text{for } M_X \gtrsim T_{max} \\ \Omega_X h^2 &\propto \langle \sigma v \rangle \frac{T_{re}^{\frac{7+3w_\phi}{1+w_\phi}}}{M_X^{\frac{9-7w_\phi}{2(1+w_\phi)}}} \propto \frac{\langle \sigma v \rangle}{M_X^{\frac{9-7w_\phi}{2(1+w_\phi)}}} \left[\left(\frac{a_0 T_0}{k} \right) H_k e^{-N_k} e^{-N_{re}} \right]^{\frac{7+3w_\phi}{1+w_\phi}} \quad \text{for } T_{max} > M_X > T_{re} \\ \Omega_X h^2 &\propto \langle \sigma v \rangle M_X T_{re} \propto \langle \sigma v \rangle M_X \left(\frac{a_0 T_0}{k} \right) H_k e^{-N_k} e^{-N_{re}} \quad \text{When } M_X < T_{re}. \end{aligned} \quad (36)$$

Depending upon the mass of the dark matter we can clearly see the behavior of the dark matter parameter space intimately connected to the CMB scale and the associated temperature. To this end let us also count the number of independent parameter of our study. At the current epoch of our universe, we have two observables corresponding to the CMB anisotropic power spectrum and the dark matter abundance. Based on our assumption that the radiation and the dark matter are produced through inflaton decay, we have four parameters $(\phi_*, \langle \sigma v \rangle, \Gamma, M_X)$ during reheating. Therefore, given the initial condition set by the CMB on the inflaton and present dark matter abundance, we have two independent parameters (ϕ_*, M_X) left. With this strategy, we will study the Boltzmann equations during reheating and show how for a given set (ϕ_*, M_X) , we can constrain the dark matter annihilation cross-section through the CMB anisotropy.

1. Numerical results, constraints on the model

With the help of formalism described above, in this section, we would like to describe the constraints on various parameters of our model. As we have already discussed, for a particular model with n value, we have two independent parameters (ϕ_*, M_X) . The first and foremost point we would like to make is that the production of dark matter does not have much effect on the

determination of reheating temperature for all the models. However it is important to mention that specifically for the dark matter mass $M_X > T_{re}$, it is the reheating period which plays important role in determining the present dark matter abundance. In the following we have considered $n = 2, 4, 6, 8$ and three sample values of $\phi_* = 10, 1, 0.1$ in unit of Planck mass. Before we go to the quantitative discussion, let us point out the general results for all the models and there generic behavior for different parameters values. For the class of minimal models we discussed, the spectral index is expressed as

$$n_s^k \simeq 1 - \frac{2n(n+1)M_p^2}{\phi_*^2} \frac{1}{\tilde{\phi}_k^{n+2}} \quad (37)$$

Where, ϕ_k is the field value of a mode k at horizon crossing. This equation can be inverted to find ϕ_k in terms of n_s . Once, we know this relation all the quantities such as tensor-to-scalar ratio r , the efolding number between the horizon crossing of a particular mode k and the end of inflation N_k and the parameter m (for $n \neq 4$) or λ (for $n = 4$) can be found in terms of n_s and ϕ_* .

For $n < 4$, in $(n_s \text{ vs } N_{re})$ plot, our generic observation is that with the increasing n_s , the reheating efolding number N_{re} is decreasing as seen in fig.(2a), and as a consequence reheating temperature T_{re} is increasing shown in fig.(2b). This behavior suggest the existence of maximum reheating temperature T_{re}^{max} thereby providing the maximum allowed scalar spectral index n_s^{max} . This also indicates the instantaneous reheating for $n_s = n_s^{max}$. On the other hand for $n > 4$, what we observed is the opposite that is the reheating efolding number N_{re} is increasing as seen in fig.(6a), and as a consequence reheating temperature T_{re} is decreasing with n_s , as shown in fig.(6b). The maximum reheating temperature corresponding to a minimum possible n_s^{min} . In this case the instantaneous reheating occurs for $n_s = n_s^{min}$. This feature also have been observed in work [10], with the effective single fluid equation of state formalism. However, another important fact that we observed is the existence of possible maximum reheating temperature $T_{re}^{max} \simeq 10^{15}$ GeV irrespective the of different parameters in our models. For all values of n and ϕ_* , we found this temperature has an important connection with the CMB anisotropy. As we have already described in detail, by tuning the value of ϕ_* , we can go from large field to small field inflation model. However, our prediction of T_{re}^{max} appeared to be independent of the inflation model. We will elaborate on this issue in our future publication. Never the less, from the numerical fitting we express the reheating temperature T_{re} in terms of spectral index n_s with the following approximate relation,

$$\log_{10}(T_{re}) \simeq Q_p [A + B(n_s - 0.962) + C(n_s - 0.962)^2]. \quad (38)$$

Where, the dimensionless constants $A = 4$, $B = 1.5 \times 10^3$ and $C = 6 \times 10^4$ for $n = 2$, $A = 20$, $B = -5 \times 10^3$ and $C = -1.5 \times 10^4$ for $n = 6$ and $A = 20$, $B = -3 \times 10^3$ and $C = -1.5 \times 10^4$

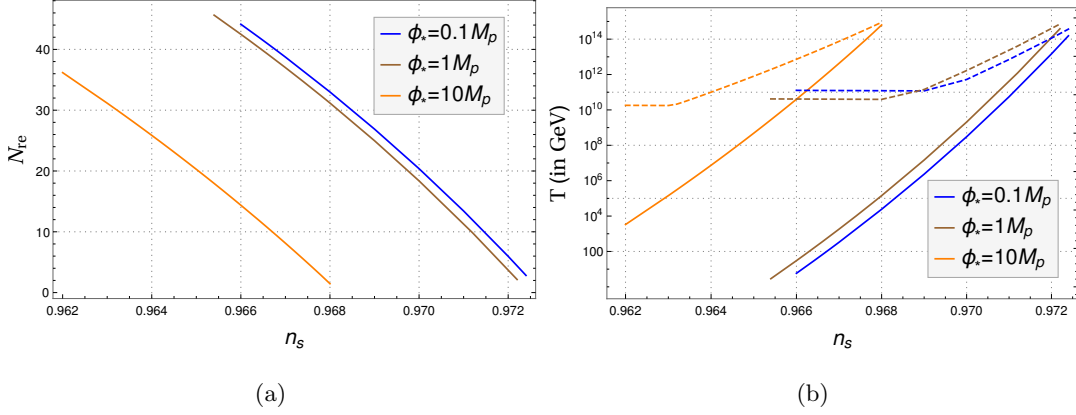


FIG. 2: Evolution of (a) Reheating e-folding number N_{re} during reheating and (b) the reheating temperature T_{re} (solid lines) and the maximum temperature T_{max} (dotted lines) with respect to n_s for $n = 2$ for three different values of ϕ_* . If one extrapolates the solid and dotted lines, one will have maximum reheating temperature $T_{re}^{max} \simeq 10^{15}$ GeV. All the plots are independent of dark matter masses for a set of given initial condition.

$n = 8$. The proportionality constant Q_p is ϕ_* dependent constant. From the above eqs.(38) and (40), we can clearly build an important connection between the dark matter abundance and the CMB anisotropy which is directly connected to the scalar spectral index n_s . In the next section, we will present our detail numerical results.

2. Results and constraints: Model n=2

This is similar to the usual quadratic chaotic model. However, as we have seen before the new parameter ϕ_* controls the behavior of cosmological parameters in a significant way. From the Fig.(2.a-b) we see the behavior of N_{re} and (T_{re}, T_{max}) in terms of n_s . It is evident that the allowed region of n_s shifts towards lower values as we increase ϕ_* , which in fact resembles the usual chaotic inflation. For $\phi_* < M_p$ we have small field inflation and the values of (n_s, r) are in agreement with the observation. For these small field models, therefore, within the 1σ range

Model parameters and associated constraints on dark matter parameters for n=2

TABLE II: $\phi_* = 0.1 M_p$

TABLE III: $\phi_* = 1 M_p$

TABLE IV: $\phi_* = 10 M_p$

n_s	N_{re}	$T_{re}(GeV)$	$\langle\sigma v\rangle GeV^{-2}$ $M_X(200TeV)$	n_s	N_{re}	$T_{re}(GeV)$	$\langle\sigma v\rangle GeV^{-2}$ $M_X(200TeV)$	n_s	N_{re}	$T_{re} GeV$	$\langle\sigma v\rangle GeV^{-2}$ $M_X(200TeV)$
0.966	44	5.8	<i>unitarity</i>	0.966	42.5	30.1	<i>unitarity</i>	0.962	36	3.3×10^3	3×10^{-24}
0.968	33	2.4×10^4	3×10^{-30}	0.968	31	1.4×10^5	6×10^{-34}	0.964	26	7.4×10^6	2×10^{-36}
0.970	20	3×10^8	5×10^{-38}	0.970	18	2×10^9	2×10^{-40}	0.966	14	4×10^{10}	4×10^{-40}
0.972	6	1.5×10^{13}	1×10^{-42}	0.9722	2	3.8×10^{14}	3×10^{-44}	0.968	1.5	6×10^{14}	3×10^{-44}

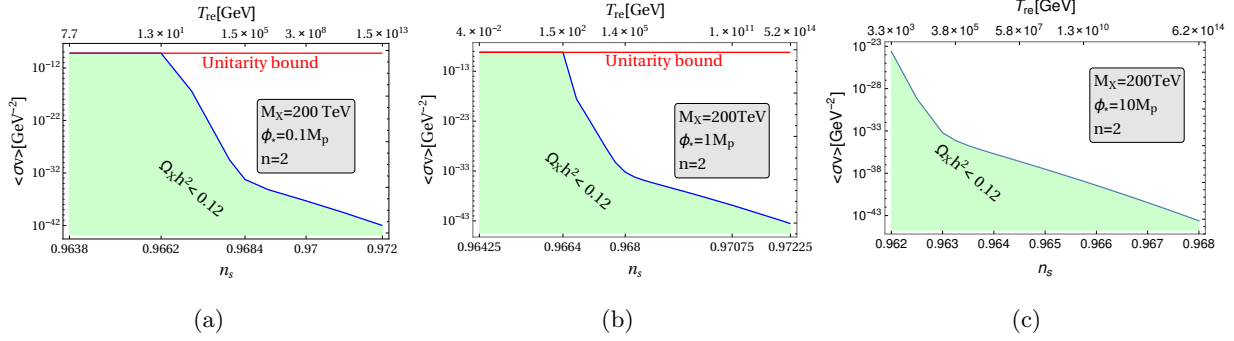


FIG. 3: ($\langle\sigma v\rangle$ vs n_s) were plotted for three values of ϕ_* and $n = 2$. The blue line with green shaded region corresponds to dark matter abundance $\Omega_X h^2 \leq 0.12$. We consider three possible values of ϕ_* . For all the cases we have chosen a dark matter mass $M_X = 200 \text{ TeV}$. Red horizontal line corresponds unitarity bound described in the main text.

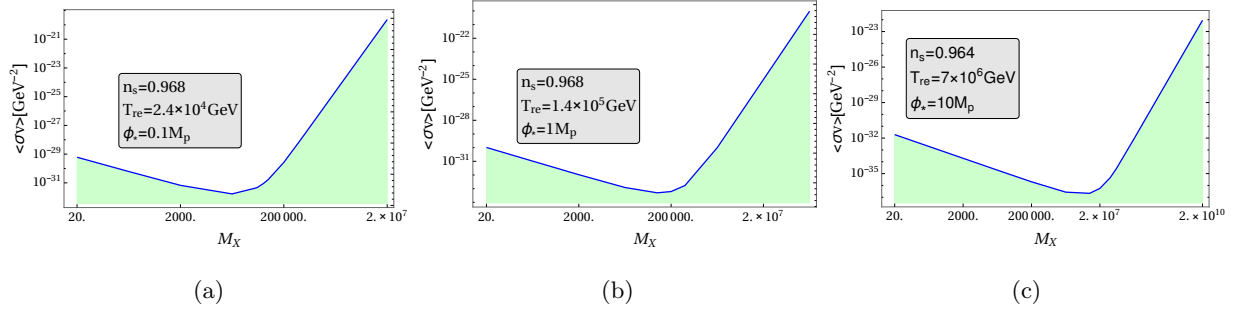


FIG. 4: ($\langle\sigma v\rangle$ vs M_X) were plotted for three values of ϕ_* and $n = 2$. Depending upon the available ranges of temperature within the 1σ range of n_s , we have considered three possible values of n_s . Minimum of the blue curve corresponds to the equality $M_X = T_{re}$. It is obvious that at this point the required value of the cross-section is minimum for a given abundance $\Omega_X h^2 = 0.12$

of n_s , very small reheating temperature can be achieved. For example at the central value of $n_s = 0.968$, reheating temperature turned out to be $10^4 \sim 10^5 \text{ GeV}$ for $\phi_* = (1, 0.1)M_p$, whereas for $\phi_* = 10M_p$, reheating temperature is very high $\sim 10^{14} \text{ GeV}$. These fact can be seen from sample values given in the Tab.III A 2 and also from the fig.(2.a-b). The lower limit of the value of n_s is set from BBN constraints[45–48], which is $T_{re} \sim 0.1 \text{ GeV}$. On the other hand, we can see from the all the plots as well as from the data tables, there exists a maximum temperature(corresponding to the instantaneous reheating) irrespective of the value of the scale ϕ_* .

In addition to the one to one correspondence between n_s and T_{re} , we simultaneously get constraints on the dark matter parameter space as shown in fig.(3), and fig.(4). We have chosen a sample dark matter mass $M_X = 200 \text{ TeV}$. It is clear that once n_s is fixed, for a given (ϕ_*, M_X) , the scattering cross-section is also fixed. Therefore, within the 1σ range of n_s , the dark matter cross-

section $\langle\sigma v\rangle$ is bounded given the value of dark matter abundance $\Omega_X h^2 = 0.12$. More importantly depending upon the values of (M_X, n_s) the freeze-in will occur in three different regimes as we have already described in detail and also can be observed in the change of slopes of blue curves as a function of n_s as shown in Figs.(3-4). From our analysis, we see that for a fixed dark matter mass, annihilation cross-section increases with decreasing n_s . However, as the cross section can not be arbitrarily large, the unitarity limit on $\langle\sigma v\rangle_{MAX} = 8\pi/M_X^2$ restricts the allowed region of n_s at its lowest value. From fig.(3.a-b) when, $\phi_* = 0.1M_p, 1M_p$ the production of dark matter particle of mass $200TeV$ for lower n_s regime is forbidden due to the unitarity bound (shown as red line). The lowest possible value of n_s turns out to be around 0.9664 and the highest value $n_s^{max} \simeq 0.968$ for $\phi_* = 10M_p$. For $\phi_* = (0.1, 1)M_p$, it turned out that $n_s^{max} \simeq 0.972$ as has already been noted before, depend upon the maximum attainable temperature for the model. This important constraint on the value of n_s coming from dark matter sector could be very important to understand and needs further study. Figs.(4.d-f) illustrates the conventional behavior of annihilation cross-section in terms of dark matter mass. However, an important point we would like to make again is that depending upon the value of inflationary power spectrum n_s or CMB anisotropy, we can shed light on the possible production mechanism given the value of dark matter mass.

3. Results and constraints: **Model n=4**

This is a very special case out of all the models. One of the main reasons is that for $n = 4$, the inflaton behaves like radiation during reheating with the equation of state parameter $\omega_\phi = 1/3$. It is known that during reheating if we consider the effective equation of state to be radiation like, then distinguishing the reheating period and the radiation dominated period becomes very difficult as can be seen from the schematic diagram fig.(1). This very fact makes the reheating parameters (N_{re}, T_{re}) indeterministic which has been observed in [10]. However, in our analysis, we managed to resolve this fact by considering the explicit decay of inflaton into the analysis. Therefore, even though the inflaton equation of state is radiation like, the effective single fluid equation of state during reheating will not be exactly radiation like rather it has complicated time dependence, expressed as

$$w_{eff} = \left\langle \frac{3p_\phi + \rho_{rad}}{3(\rho_\phi + \rho_{rad} + \rho_X)} \right\rangle. \quad (39)$$

However, in deriving the above equation of state we assumed the perturbative decay of inflation. Keeping this fact in mind, our result for $n = 4$ is given in the fig.(5). It clearly shows the stiffness of the curve which can be attributed to the fact that effective equation of state varies very close

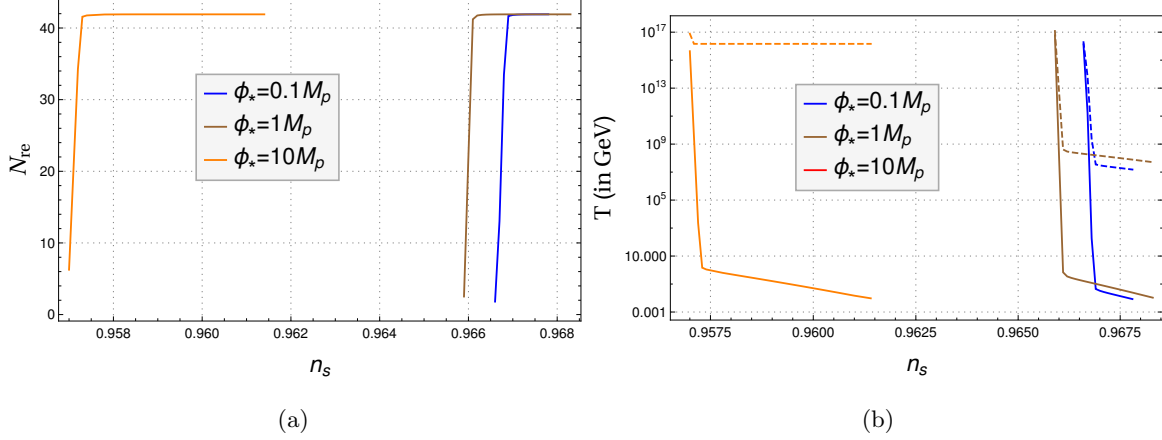


FIG. 5: Evolution of (a) Reheating e-folding number N_{re} during reheating and (b) the reheating temperature T_{re} (solid lines) and the maximum temperature T_{max} (dotted lines) with respect to n_s for $n = 4$ for three different values of ϕ_* . We have will same $T_{re}^{max} \simeq 10^{15}$ GeV.

to $1/3$. There exist some flat regions as we lower the value of n_s , which we think should be our numerical artefact. Therefore, if we discard that flat region, $n = 4$ model predicts a precise value of scalar spectral index n_s , however, N_{re}, T_{re} become very sensitive to slight variation of it. As we can see from the fig.(5), the scalar spectral index assumes $n_s \simeq (0.9575, 0.966, 0.967)$ values for $\phi_* = (10, 1, 0.1)M_p$. Therefore, an important conclusion we can arrive from our analysis that super-Planckian values of $\phi_* > 1M_p$ are disfavored as long as n_s measurement is concerned.

4. Results and constraints: Model n=6

As we know all the usual power law inflationary models are large field and consequently predicts large r value. However, because of new scale ϕ_* , we were able to make our model perfectly compatible with the observation for even stiffer model such as $n = 6$ and $n = 8$. In this

Model parameters and associated constraints on dark matter parameters for n=6

TABLE V: $\phi_* = 0.1M_p$

TABLE VI: $\phi_* = 1M_p$

TABLE VII: $\phi_* = 10M_p$

n_s	N_{re}	$T_{re}(GeV)$	$\langle\sigma v\rangle GeV^{-2}$ $M_X(10^{11}GeV)$	n_s	N_{re}	$T_{re}(GeV)$	$\langle\sigma v\rangle GeV^{-2}$ $M_X(10^{11}GeV)$	n_s	N_{re}	$T_{re}(GeV)$	$\langle\sigma v\rangle GeV^{-2}$ $M_X(10^{11}GeV)$
0.9678	3	4×10^{13}	3×10^{-49}	0.9682	2	1×10^{14}	9×10^{-50}	0.9632	2	1.9×10^{14}	6×10^{-50}
0.968	5	2×10^{12}	7×10^{-48}	0.969	14	3×10^8	1×10^{-36}	0.964	11	6×10^9	4×10^{-41}
0.969	20	2×10^5	9×10^{-34}	0.970	29	10.58	unitarity	0.965	23	8.8×10^3	unitarity
0.9698	32	0.2	6×10^{-22}	0.972	32	0.3	unitairty	0.9656	30	2	unitarity

sub-section we summarized all our analysis in the figs.(6,7,8) and the following tables (III A 4) for $n = 6$.

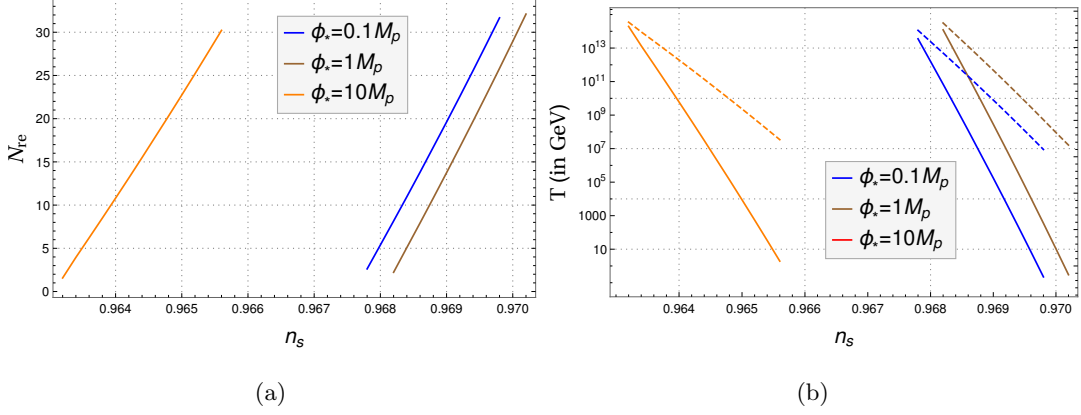


FIG. 6: Evolution of (a) Reheating e-folding number N_{re} during reheating and (b) the reheating temperature T_{re} (solid lines) and the maximum temperature T_{max} (dotted lines) with respect to n_s for $n = 6$ for three different values of ϕ_* . One clearly see the change of slop in compared to $n < 4$ models. However, we observed maximum reheating temperature to the same $T_{re}^{max} \simeq 10^{15}$ GeV.

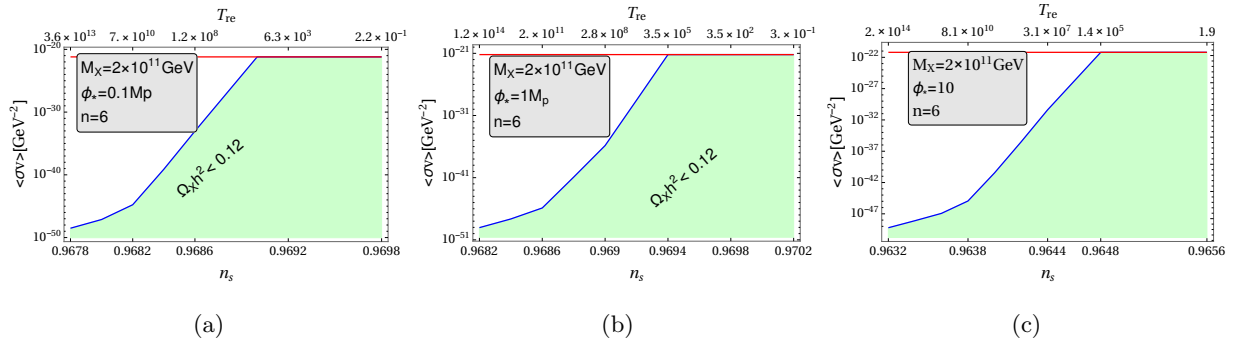


FIG. 7: ($\langle\sigma v\rangle$ vs n_s) were plotted for three values of ϕ_* and $n = 6$. For all the cases we have chosen a dark matter mass $M_X = 2 \times 10^{11}$ GeV.

Important difference with $n < 4$ models turned out to be the slope of (n_s vs T_{re}) and (n_s vs N_{re}) curve. This has also been explained in the schematic diagram fig.(1). This is coming from the stiff equation of state of the oscillating inflaton $w_\phi = (n - 2)/(n + 2) = 1/2 > 1/3$. The duration of reheating period (N_{re}) increases with increasing n_s . Therefore, unlike $n < 4$ models, corresponding to the maximum reheating temperature we have minimum possible values of n_s .

5. Results and constraints: Model $n=8$

For $n = 8$, the qualitative behavior of all the plots will be same as $n = 6$. Therefore we summarize all our results in the table-III A 5 and the respective plots. Important to see that very small reheating temperature can be reached in this model. At the central value of $n_s = 0.968 \pm 0.006$, we see reheating temperature could be $10^4 \sim 10^5$ GeV given in the tab.(III A 5). The lowest value of

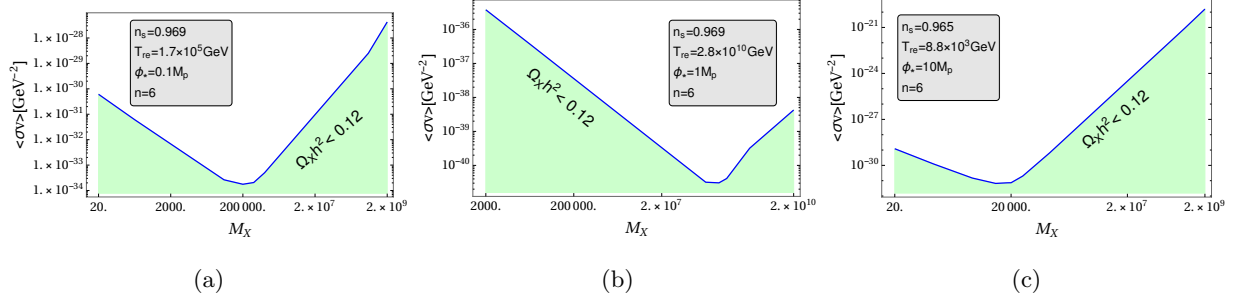


FIG. 8: $(\langle\sigma v\rangle vs M_X)$ were plotted for three values of ϕ_* and $n = 6$. General descriptions of the plots are same as before.

n_s can be set from the minimum possible reheating temperature coming from BBN constraints[45–48], which is $T_{re} \sim 0.1 \text{ GeV}$.

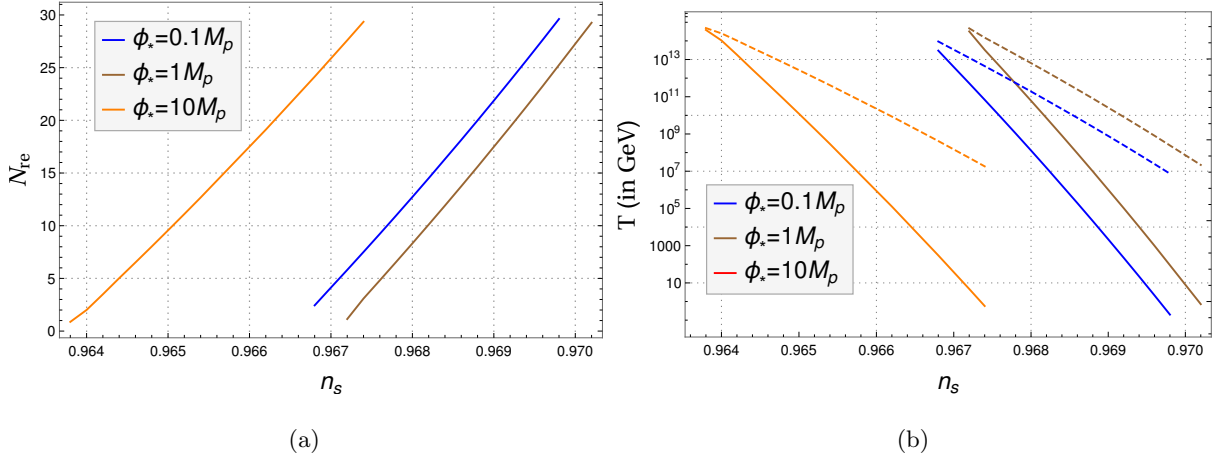


FIG. 9: Evolution of (a) Reheating e-folding number N_{re} during reheating and (b) the reheating temperature T_{re} (solid lines) and the maximum temperature T_{max} (dotted lines) with respect to n_s for $n = 8$ with the same behavior as $n = 6$.

Model parameters and associated constraints on dark matter parameters for $n=8$

TABLE VIII: $\phi_* = 0.1 M_p$

TABLE IX: $\phi_* = 1 M_p$

TABLE X: $\phi_* = 10 M_p$

n_s	N_{re}	$T_{re}(\text{GeV})$	$\langle\sigma v\rangle \text{GeV}^{-2}$ $M_X(10^{11} \text{ GeV})$	n_s	N_{re}	$T_{re}(\text{GeV})$	$\langle\sigma v\rangle \text{GeV}^{-2}$ $M_X(10^{11} \text{ GeV})$	n_s	N_{re}	$T_{re}(\text{GeV})$	$\langle\sigma v\rangle \text{GeV}^{-2}$ $M_X(10^{11} \text{ GeV})$
0.9668	2	3×10^{13}	4×10^{-49}	0.9672	1	3×10^{14}	4×10^{-50}	0.9638	1	4×10^{14}	3×10^{-50}
0.968	13	1×10^8	7×10^{-35}	0.968	8	6×10^{10}	2×10^{-45}	0.964	2	1×10^{14}	1×10^{-49}
0.969	22	2×10^3	<i>unitarity</i>	0.9692	19	1×10^5	<i>unitarity</i>	0.965	10	1×10^{10}	3×10^{-43}
0.9698	30	0.2	<i>unitarity</i>	0.9702	29	0.72	<i>unitarity</i>	0.9674	29	1	<i>unitarity</i>

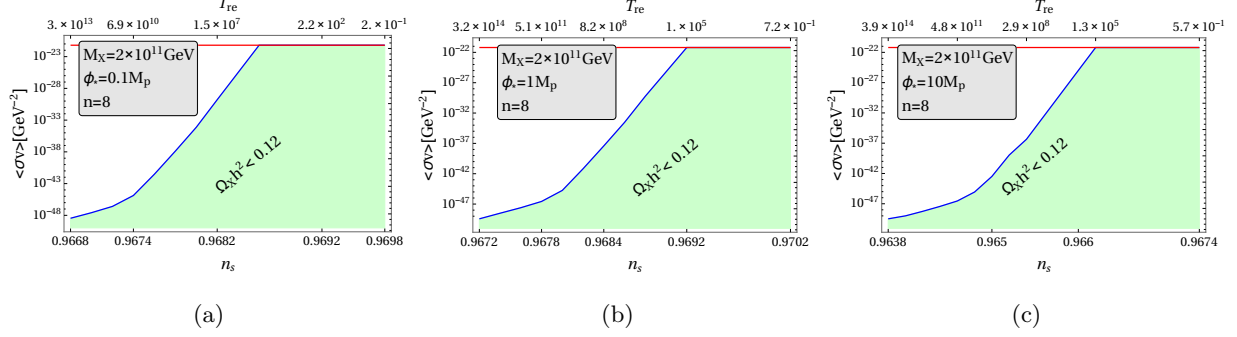


FIG. 10: ($\langle\sigma v\rangle$ vs n_s) were plotted for $n = 8$. Descriptions are same as previous plots. For all the plots we have chosen dark matter mass $M_X = 2 \times 10^{11} \text{ GeV}$.

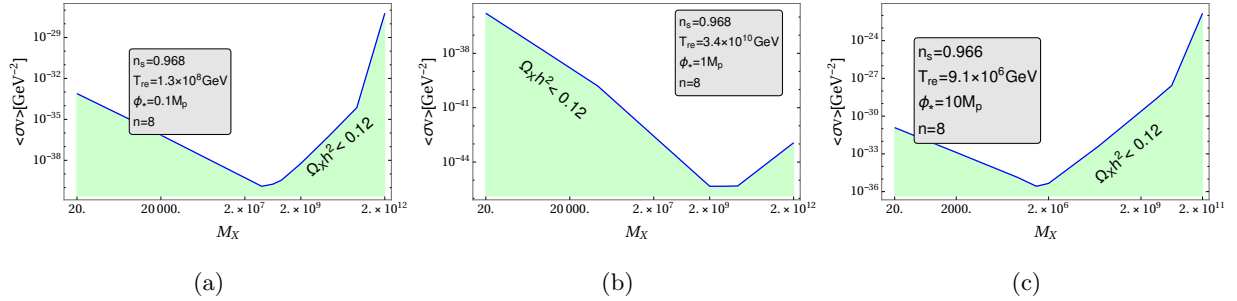


FIG. 11: ($\langle\sigma v\rangle$ vs M_X) were plotted for $n = 8$.

IV. CONCLUSIONS AND FUTURE DIRECTIONS

In this paper, we have done the reheating constraint analysis in detail for a class of inflationary models with non-standard potential [7]. Our focus was on understanding the inflation model as well as dark matter phenomenology via reheating phase. For both the analysis, the CMB plays a very important role. We, therefore, follow the formalism developed in [29] where the dark matter parameter space is constrained via CMB anisotropy and the reheating dynamics. Constraints on dark matter parameter space are dependent upon the specific model of inflation. As mentioned throughout the paper, in our recent work on minimal inflationary cosmologies we had discussed in detail the role of inflationary scale ϕ_* . By tuning it, we also obtained both high scale as well as low scale inflations which are observationally viable. In this paper we considered those inflationary models and further extended our work on understanding the role of that scale on the reheating phase as well as on dark matter phenomenology.

As we all know, the reheating phase, which is relatively less understood due to lack of direct observables, has potential to explain many unanswered questions related to dark matter, baryogenesis etc. In this paper, we have studied in detail the reheating period considering the perturbative

Summary table for central value of n_s with dark matter mass taken to be $M_X = 200$ TeV

TABLE XI: $\phi_* = 0.1M_p$

n	N_{re}	$T_{re}(GeV)$	$\langle\sigma v\rangle GeV^{-2}$ $M_X(200TeV)$
2	33	2.4×10^4	3×10^{-30}
4	-	-	-
6	5	1.6×10^{12}	7×10^{-42}
8	-	-	-

TABLE XII: $\phi_* = 1M_p$

n_s	N_{re}	$T_{re}(GeV)$	$\langle\sigma v\rangle GeV^{-2}$ $M_X(200TeV)$
2	31	1.4×10^5	6×10^{-34}
4	-	-	-
6	13	1.3×10^8	7×10^{-38}
8	8	6×10^{10}	2×10^{-40}

TABLE XIII: $\phi_* = 10M_p$

n	N_{re}	$T_{re}(GeV)$	$\langle\sigma v\rangle GeV^{-2}$ $M_X(200TeV)$
2	1.5	6×10^{14}	3×10^{-44}
4	-	-	-
6	-	-	-
8	-	-	-

decay of inflaton into radiation and radiation into dark matter component. One of the important findings from our analysis is the existence of maximum reheating temperature $T_{re}^{max} \simeq 10^{15}$ GeV, which is independent of large or small scale inflation model. Therefore, it is the CMB scale which dictates the value of maximum possible reheating temperature. Corresponding to that maximum T_{re} , we also have either maximum possible n_s^{max} for all the models with $n < 4$ or minimum possible n_s^{min} for models with $n > 4$. This fact can be easily understood from the illustration in fig.1. As we have already emphasized the goal was to connect the inflation, reheating phase with the CMB anisotropy and the dark matter abundance. Therefore, we further study how the inflationary scalar spectral index fixes the dark matter annihilation cross-section for a given mass of the dark matter once we specify the model. Here is our main findings which tells us how uniquely we can constrain the dark matter parameter space $(M_X, \langle\sigma v\rangle)$, through the following important relations,

$$\begin{aligned}
\Omega_X h^2 &\propto \langle\sigma|v\rangle M_X^4 Exp \left[-\frac{E(w_\phi)M_X}{T_{max}} \right] \quad \text{for } M_X \gtrsim T_{max} \\
\Omega_X h^2 &\propto \frac{\langle\sigma v\rangle}{M_X^{\frac{2(1+w_\phi)}{9-7w_\phi}}} \left[\left(\frac{a_0 T_0}{k} \right) H_k e^{-N_k} e^{-N_{re}} \right]^{\frac{7+3w_\phi}{1+w_\phi}} \quad \text{for } T_{max} > M_X > T_{re} \\
\Omega_X h^2 &\propto \langle\sigma v\rangle M_X \left(\frac{a_0 T_0}{k} \right) H_k e^{-N_k} e^{-N_{re}} \quad \text{When } M_X < T_{re}.
\end{aligned} \tag{40}$$

The non-trivial relation among the dark matter abundance ($\Omega_X h^2$), the general inflaton equation state (w_ϕ), CMB scale k , and mass of the dark matter M_X is our main result which has not been reported before. Here an important point we would like to emphasize again that the dark matter is produced by Freeze-in mechanism. Therefore, detailed analysis for freeze out dark matter based on our formalism will be reported elsewhere.

Nevertheless considering the central value of $n_s \sim 0.968$ as given by PLANCK our model predictions are summarized in table-IV. For $n = 4$, the e-folding number during reheating(N_{re}) and consequently the reheating temperature is highly sensitive to n_s which can also be understood from fig.1. Therefore, we left those parameters blank in the summary table. From the above

summary table we can clearly see that given the central value of $n_s = 0.968$ and dark matter mass $M_X = 200$ TeV, few models can be ruled out based on the values of the model parameters for which prediction will be out of 1σ range of n_s given by PLANCK. On the other hand, if one considers n_s within the given range of PLANCK, we can give a bound on the possible range of values of annihilation cross-section for a given mass. An Important conclusion that we can make is that once the CMB anisotropy measurement fixes the value of n_s , we can completely fix the dark matter annihilation cross-section for a given mass considering the perturbative reheating process. Therefore, it is very important to pinpoint the actual value of n_s in the future experiment. Understanding the dark matter phenomenology is one of the important challenges in the particle physics community. Therefore, our formalism and present analysis may shed some light on this subject. The important assumption of our analysis is the perturbative reheating. It is well known that the non-perturbative effects such as parametric resonance can be very efficient that can initiate the radiation dominance within few e-folding numbers after the end of inflation. In that case the CMB will have very little information regarding the reheating phase. However, as shown in[49], incorporating interactions amongst the produced particles, the parametric resonance can be delayed and as a result we will get an extended period of reheating. The validity of the perturbative regime in the context of reheating has been considered in[36] considering the effective equation of state or in [50] considering the explicit inflaton decay. However, the issue of self-resonance still remains. It has been shown in[51, 52] that when considering the self-resonance, the homogeneous condensate will cease oscillating after a certain period, and ends up fragmenting into higher momentum modes of the inflaton field. For, certain form of the potentials, $V(\phi) \propto \phi^n$, the equation of state eventually ends up becoming $1/3$ instead of $(n - 2)/(n + 2)$. However, there is a certain period when this equation of state will be maintained and moreover, there are specific parameter range when the self-resonance will be inefficient. We are currently working on these issues of taking into account the non-perturbative effects.

Finally at the end let us point out an another important direction which we will report elsewhere. In our study we have solved for the homogeneous Boltzmann equation for all the energy components. However, it is well known that evolution of perturbation for every individual component would be extremely important to understand the small scale properties of CMB. Interestingly in our unified approach inflation and reheating dynamics control all the evolution. Therefore, any small scale CMB observables will certainly contain valuable information related to inflation. In this regard well known small scale μ -type and y -type spectral distortions of CMB are extremely important. At present those distortion parameters are tightly constrained by COBE and FIRAS

experiments, $|\mu| < 9 \times 10^5$ and $y < 1.5 \times 10^5$ [53]. However, future projected sensitivity for PIXIE [54] and PRISM [55] experiments are within $10^{-8} \sim 10^{-9}$. The standard model of particle physics interactions already predicts those spectral distortion parameters to be $\sim 10^{-8}$ [56, 57]. Keeping in mind the future experimental sensitivity, it would be extremely important to understand various other physics processes which can give rise to those distortions. Therefore, by using our unified approach we can further constrain inflation models considering those distortion parameters.

V. ACKNOWLEDGEMENT

We thank our HEP group members for their valuable comments and discussions.

-
- [1] A. H. Guth, Phys.Rev. D **23**, 347356 (1981).
 - [2] A. D. Linde, Phys. Lett. B **108**, 389393 (1982).
 - [3] A. Albrecht and P. J. Steinhardt, Phys. Rev. Lett. **48**, 12201223 (1982).
 - [4] J. Martin, C. Ringeval and V Vennin, Phys.Dark Univ. 5-6 (2014) 75-235, [[arXiv:1303.3787](#) [astro-ph.CO]].
 - [5] Planck Collaboration: P. A. R. Ade et al., Planck 2013 results. XXII. Constraints on Inflation, Astron. Astrophys. **571** (2014) A22, [[arXiv:1303.5082](#) [astro-ph.CO]]; Planck Collaboration: P. A. R. Ade et al., Planck 2015 results. XX. Constraints on Inflation, Astron. Astrophys. **594**, A20 (2016), [[arXiv:1502.02114](#) [astro-ph.CO]]; Keck Array, BICEP2 Collaborations: P. A. R. Ade et al., BICEP2 / Keck Array VI: Improved Constraints On Cosmology and Foregrounds When Adding 95 GHz Data From Keck Array, Phys. Rev. Lett. **116**, 031302 (2016), [[arXiv:1510.09217](#) [astro-ph.CO]]
 - [6] R. Kallosh and A. Linde, JCAP **1307**, 002 (2013) [[arXiv:1306.5220](#) [hep-th]]; S. Ferrara, et al, Phys. Rev. D **88**, 8, 085038 (2013) [[arXiv:1307.7696](#) [hep-th]]; R. Kallosh, A. Linde and D. Roest, JHEP **1311**, 198 (2013) [[arXiv:1311.0472](#) [hep-th]]; S. Cecotti and R. Kallosh, JHEP **1405**, 114 (2014) [[arXiv:1403.2932](#) [hep-th]].
 - [7] D. Maity and P. Saha, [arXiv:1610.00173](#) [astro-ph.CO].
 - [8] Y. Shtanov, J. H. Traschen and R. H. Brandenberger, Phys. Rev. D **51** (1995) 5438 [[hep-ph/9407247](#)].
 - [9] L. Kofman, A. D. Linde and A. A. Starobinsky, Phys. Rev. Lett. **73** (1994) 3195 [[hep-th/9405187](#)].
 - [10] L. Dai, M. Kamionkowski and J. Wang, Phys. Rev. Lett. **113** (2014) 041302 [[arXiv:1404.6704](#) [astro-ph.CO]].
 - [11] P. Creminelli, D. Lopez Nacir, M. Simonovi, G. Trevisan and M. Zaldarriaga, Phys. Rev. D **90** (2014) no.8, 083513 [[arXiv:1405.6264](#) [astro-ph.CO]].

- [12] J. Martin, C. Ringeval and V. Vennin, Phys. Rev. Lett. **114** (2015) no.8, 081303 [[arXiv:1410.7958](#) [astro-ph.CO]].
- [13] A. de la Macorra and S. Lola, Phys. Lett. B **373**, 299 (1996) [[hep-ph/9511470](#)].
- [14] V. Domcke and J. Heisig, Phys. Rev. D **92** (2015) no.10, 103515 [[arXiv:1504.00345](#) [astro-ph.CO]].
- [15] D. Maity, Nucl. Phys. B **919** (2017) 560 [[arXiv:1606.08179](#) [hep-ph]].
- [16] K. Dimopoulos and C. Owen, Phys. Rev. D **94**, no. 6, 063518 (2016) [[arXiv:1607.02469](#) [hep-ph]].
- [17] M. Eshaghi, M. Zarei, N. Riazi and A. Kiasatpour, JCAP **1511** (2015) no.11, 037 [[arXiv:1505.03556](#) [hep-th]].
- [18] B. J. Broy, D. Coone and D. Roest, JCAP **1606** (2016) no.06, 036 [[arXiv:1604.05326](#) [hep-th]].
- [19] T. Futamase and K. i. Maeda, Phys. Rev. D **39** (1989) 399.
- [20] D. I. Kaiser, Phys. Rev. D **52** (1995) 4295 [[astro-ph/9408044](#)].
- [21] J. c. Hwang, Class. Quant. Grav. **14** (1997) 1981 [[gr-qc/9605024](#)].
- [22] N. Deruelle and M. Sasaki, Springer Proc. Phys. **137** (2011) 247 [[arXiv:1007.3563](#) [gr-qc]].
- [23] M. Postma and M. Volponi, Phys. Rev. D **90** (2014) no.10, 103516 [[arXiv:1407.6874](#) [astro-ph.CO]].
- [24] S. Pandey and N. Banerjee, [arXiv:1610.00584](#) [gr-qc].
S. Pandey, S. Pal and N. Banerjee, [arXiv:1611.07043](#) [gr-qc].
- [25] K. Bhattacharya and B. R. Majhi, [arXiv:1702.07166](#) [gr-qc].
- [26] Y. Fujii and K. Maeda, “The Scalar-Tensor Theory of Gravitation,” Cambridge University Press; (2007)
- [27] R. Kallosh, A. Linde and D. Roest, Phys. Rev. Lett. **112** (2014) no.1, 011303 [[arXiv:1310.3950](#) [hep-th]].
- [28] M. Galante, R. Kallosh, A. Linde and D. Roest, Phys. Rev. Lett. **114** (2015) no.14, 141302 [[arXiv:1412.3797](#) [hep-th]].
Phys. Rev. D **94** (2016) no.12, 123521 [[arXiv:1609.04739](#) [astro-ph.CO]].
- [29] D. Maity and P. Saha, [arXiv:1801.03059](#) [hep-ph].
- [30] J. L. Cook, E. Dimastrogiovanni, D. A. Easson and L. M. Krauss, JCAP **1504** (2015) 047 [[arXiv:1502.04673](#) [astro-ph.CO]].
- [31] J. Ellis, M. A. G. Garcia, D. V. Nanopoulos and K. A. Olive, JCAP **1507** (2015) no.07, 050 [[arXiv:1505.06986](#) [hep-ph]].
- [32] Y. Ueno and K. Yamamoto, Phys. Rev. D **93** (2016) no.8, 083524 [[arXiv:1602.07427](#) [astro-ph.CO]].
- [33] M. Eshaghi, M. Zarei, N. Riazi and A. Kiasatpour, Phys. Rev. D **93** (2016) no.12, 123517 [[arXiv:1602.07914](#) [astro-ph.CO]].
- [34] A. Di Marco, P. Cabella and N. Vittorio, Phys. Rev. D **95** (2017) no.10, 103502 [[arXiv:1705.04622](#) [astro-ph.CO]].
- [35] S. Bhattacharya, K. Dutta and A. Maharana, Phys. Rev. D **96** (2017) no.8, 083522 [[arXiv:1707.07924](#) [hep-ph]].
- [36] M. Drewes, J. U. Kang and U. R. Mun, [arXiv:1708.01197](#) [astro-ph.CO].
- [37] G. F. Giudice, E. W. Kolb and A. Riotto, Phys. Rev. D **64** (2001) 023508 [[hep-ph/0005123](#)].
- [38] Cario Cercignani and Gilberto Medeiros Kremer, The Relativistic Boltzmann Equation: Theory and Applications, Progress in Mathematical Physics (Book 22), Birkhuser; 2002 edition (April 29, 2002)

- [39] E. W. Kolb and M. S. Turner, *Front. Phys.* **69** (1990) 1.
- [40] D. J. H. Chung, E. W. Kolb and A. Riotto, *Phys. Rev. D* **60** (1999) 063504 [[hep-ph/9809453](#)].
- [41] R. Allahverdi and M. Drees, *Phys. Rev. Lett.* **89** (2002) 091302 doi:10.1103/PhysRevLett.89.091302 [[hep-ph/0203118](#)].
- [42] R. Allahverdi and M. Drees, *Phys. Rev. D* **66** (2002) 063513 doi:10.1103/PhysRevD.66.063513 [[hep-ph/0205246](#)].
- [43] P. S. Bhupal Dev, A. Mazumdar and S. Qutub, *Front. in Phys.* **2** (2014) 26 [[arXiv:1311.5297](#) [hep-ph]].
- [44] L. J. Hall, K. Jedamzik, J. March-Russell and S. M. West, *JHEP* **1003** (2010) 080 [[arXiv:0911.1120](#) [hep-ph]]; T. Tenkanen, *JHEP* **1609** (2016) 049 [[arXiv:1607.01379](#) [hep-ph]]. M. Heikinheimo, T. Tenkanen, K. Tuominen and V. Vaskonen, *PoS ICHEP* **2016** (2016) 825 [[arXiv:1611.04951](#) [astro-ph.CO]]; N. Bernal, M. Heikinheimo, T. Tenkanen, K. Tuominen and V. Vaskonen, *Int. J. Mod. Phys. A* **32** (2017) no.27, 1730023 [[arXiv:1706.07442](#) [hep-ph]];
- [45] M. Kawasaki, K. Kohri and N. Sugiyama, *Phys. Rev. Lett.* **82** (1999) 4168 [[astro-ph/9811437](#)].
- [46] M. Kawasaki, K. Kohri and N. Sugiyama, *Phys. Rev. D* **62** (2000) 023506 [[astro-ph/0002127](#)].
- [47] G. Steigman, *Ann. Rev. Nucl. Part. Sci.* **57** (2007) 463 [[arXiv:0712.1100](#) [astro-ph]].
- [48] B. D. Fields, P. Molaro and S. Sarkar, *Chin. Phys. C* **38** (2014) 339 [[arXiv:1412.1408](#) [astro-ph.CO]].
- [49] J. Garcia-Bellido, D. G. Figueroa and J. Rubio, *Phys. Rev. D* **79** (2009) 063531 [[arXiv:0812.4624](#) [hep-ph]].
- [50] D. Maity, [arXiv:1709.00251](#) [hep-th].
- [51] K. D. Lozanov and M. A. Amin, *Phys. Rev. Lett.* **119** (2017) no.6, 061301 [[arXiv:1608.01213](#) [astro-ph.CO]].
- [52] K. D. Lozanov and M. A. Amin, *Phys. Rev. D* **97** (2018) no.2, 023533 [[arXiv:1710.06851](#) [astro-ph.CO]].
- [53] D. J. Fixsen, E. S. Cheng, J. M. Gales, J. C. Mather, R. A. Shafer, and E. L. Wright, *Astrophys. J.* **473**, 576 (1996).
- [54] A. Kogut et al., The Primordial Inflation Explorer (PIXIE): A Nulling Polarimeter for Cosmic Microwave Background Observations, *JCAP* **1107**, 025 (2011) [[arXiv:1105.2044](#)].
- [55] PRISM Collaboration, P. Andre et al., PRISM (Polarized Radiation Imaging and Spectroscopy Mission): A White Paper on the Ultimate Polarimetric Spectro-Imaging of the Microwave and Far-Infrared Sky, [arXiv:1306.2259](#) [astro-ph.CO].
- [56] J. Chluba and R. A. Sunyaev, *Mon. Not. R. Astron. Soc.*, **419**, 1294 (2012) [[arXiv:1109.6552](#)];
- [57] H. Tashiro, *PTEP*, **2014**, (2014) no. 6, 06B107 ; J. Chluba, J. Hamann, and S. P. Patil, *Int. J. Mod. Phys. D* **24**, 1530023 (2015) [[arXiv:1505.01834](#)].